Exploiting Temporal Collateral Sensitivity in Tumor Clonal Evolution

HHS Public Access

Author manuscript

Cell. Author manuscript; available in PMC 2017 March 24.

Published in final edited form as:

Cell. 2016 March 24; 165(1): 234–246. doi:10.1016/j.cell.2016.01.045.

Exploiting temporal collateral sensitivity in tumor clonal evolution

Boyang Zhao[1,2], **Joseph C. Sedlak**[7], **Raja Srinivas**[4,5], **Pau Creixell**[2], **Justin R. Pritchard**[2,3,8], **Bruce Tidor**[4,5,6], **Douglas A. Lauffenburger**[2,3,4,*], and **Michael T. Hemann**[2,3,*]

[1]Computational and Systems Biology Program, Massachusetts Institute of Technology, Cambridge, MA 02139

[2]The David H. Koch Institute for Integrative Cancer Research, Massachusetts Institute of Technology, Cambridge, MA 02139

[3]Department of Biology, Massachusetts Institute of Technology, Cambridge, MA 02139

[4]Department of Biological Engineering, Massachusetts Institute of Technology, Cambridge, MA 02139

[5]Computer Science and Artificial Intelligence Laboratory, Massachusetts Institute of Technology, Cambridge, MA 02139

[6]Department of Electrical Engineering and Computer Science, Massachusetts Institute of Technology, Cambridge, MA 02139

[7]Harvard/MIT MD-PhD Program, Harvard Medical School, Boston, MA 02115

SUMMARY

The prevailing approach to addressing secondary drug resistance in cancer focuses on treating the resistance mechanisms at relapse. However, the dynamic nature of clonal evolution, along with potential fitness costs and cost compensations, may present exploitable vulnerabilities; a notion that we term ‘temporal collateral sensitivity’. Using a combined pharmacological screen and drug resistance selection approach in a murine model of Ph+ acute lymphoblastic leukemia, we indeed find that temporal and/or persistent collateral sensitivity to non-classical BCR-ABL1 drugs arises in emergent tumor subpopulations during the evolution of resistance toward initial treatment with BCR-ABL1 targeted inhibitors. We determined the sensitization mechanism via genotypic, phenotypic, signaling, and binding measurements in combination with computational models, and demonstrated significant overall survival extension in mice. Additional stochastic mathematical

*Correspondence and requests for materials should be addressed to D.A.L (lauffen@mit.edu) and M.T.H (hemann@mit.edu).
[8]Present address: ARIAD Pharmaceuticals, Inc., Cambridge, MA 02139

Accession numbers

RNA-seq data have been deposited in Gene Expression Omnibus under the accession number GSE72910.

Further details on experimental procedures and computational methods can be found in Supplemental Information.

AUTHOR CONTRIBUTIONS

B.Z., D.A.L., and M.T.H. designed research. B.Z. performed *in vitro* and *in vivo* experiments and computational modeling. J.C.S. made contributions to the ODE mathematical model. R.S. and B.T. performed small molecule docking. P.C. performed computational analyses using KINspect to evaluate consequences of mutants on kinase specificity. J.R.P. provided reagents and conceptual contributions toward research design and data analysis. B.Z., D.A.L., and M.T.H. analyzed data and wrote the manuscript with input from all authors.

models and small molecule screens extended our insights, indicating the value of focusing on evolutionary trajectories and pharmacological profiles to identify new strategies to treat dynamic tumor vulnerabilities.

INTRODUCTION

Collateral sensitivity describes a type of synthetic lethality that has been explored in cancer and infectious diseases for over forty years. Intrinsic to this concept is an evolutionary trade-off – where resistance toward a drug or drugs comes at the expense of sensitivity to other drugs. This phenomenon has spurred efforts to screen chemoresistant cell lines against a panel of drugs for collateral sensitivity and resistance (Jensen et al., 1997; Rickardson et al., 2006). Additionally, several recent high-throughput evolutionary experiments have attempted to build a collateral sensitivity networks using *E. coli* treated with 10–20 antibiotics, with the goal of designing drug cycling regimens that select against drug resistance (Imamovic and Sommer, 2013; Lázár et al., 2014). Evolutionary trade-offs have also been investigated for drug combinations (Hill et al., 2015; Kim et al., 2014), and have been utilized for potential control of subsequent tumor cell evolutionary trajectories (Chen et al., 2015; Zhao et al., 2014).

In the field of cancer treatment, drug resistance studies have traditionally been focused on mechanism of resistance at the end of drug selection experiments. However, our understanding of intratumoral heterogeneity and clonal selection is increasingly revealing that tumor evolution is a dynamic process. Recent sequencing efforts have revealed extensive branched clonal evolution during tumor progression (Fisher et al., 2013; Gerlinger et al., 2012), and matched samples prior and post treatment often enrich a pre-existing subclone toward dominance at relapse (Ding et al., 2012; Misale et al., 2012). Such studies have also been recapitulated in *in vitro* settings with pre-existing resistant subclones estimated in one study at 0.001–0.05% of the parental population (Bhang et al., 2015).

As with the bacterial antibiotics system, these evolutionary processes can sometimes present evolutionary trade-offs. Fitness costs of resistance have been extensively studied in bacteria, with findings that reduced fitness can in some cases concomitantly lead to acquisition of subsequent mutation(s) for cost compensation (Andersson and Hughes, 2010). Therefore, we posited that there could be intermediate states during tumor clonal evolutionary progression that present persistent or temporal vulnerabilities. A conceptual illustration of our hypothesis is shown in Figure 1, where tumor genotype characteristics are represented on two abscissa axes of variation, such as could be the case for two independent gene mutations. “Fitness” on the ordinate axis is essentially the reciprocal of efficacy under whichever environmental conditions – such as a drug treatment – the tumor is dynamically evolving in. As a tumor becomes increasingly populated by cells resistant to treatment with an initial drug A (up-hill mountain in panel A), there can be drugs from distinct drug categories that are inactive (Fig 1B) or collaterally sensitizing to the terminal resistant stage of clonal evolution (Fig 1C). However, it is also conceivable that certain genotype variations (e.g. on-target mutations and/or alterations in signaling pathways) would render at least a proportion of the evolving tumor more susceptible to a different drug D (downhill valley in panel D). This situation in

theory could lead to a treatment regimen with drug D following drug A during a restricted time-window producing overall increased treatment efficacy – a notion that can be termed ‘temporal collateral sensitivity’.

In this study, we report an experimental validation of temporal collateral sensitivity in a murine preclinical model of Philadelphia chromosome (Ph)-positive acute lymphoblastic leukemia (ALL). Current BCR-ABL1 (the fusion protein generated by the Philadelphia chromosome) tyrosine kinase inhibitors (TKIs) have dramatically improved the prognosis for chronic myeloid leukemia and to some degree Ph+ ALL. However, a major resistance mechanism for relapsed patients is the on-target BCR-ABL1 dependent mutations in the kinase domain, including the most common gatekeeper T315I mutation that confers resistance to four of the five FDA-approved drugs (O’Hare et al., 2012; Soverini et al., 2006). Even then, compound mutations (i.e. more than one mutation in the same BCR-ABL1 allele) remain a challenge (Khorashad et al., 2013; Zabriskie et al., 2014). Through a joint drug resistance selection and pharmacological profile, here we discover a particularly strong and robust collateral sensitivity to non-classical BCR-ABL1 inhibitors (i.e. not known and used to target BCR-ABL1) crizotinib, foretinib, cabozantinib, and vandetanib for Ph+ ALL cells at intermediate stages of clonal evolution. We show that this effect is driven by the occurrence of the BCR-ABL1 V299L single mutation, before its continued evolution toward V299L compound mutants. Molecular studies suggest an on-target ABL1 inhibition exclusive to V299L (and a subset of V299L compound mutants). Most importantly, the mechanism is distinct from drug synergy as a result of temporal cellular rewiring, but rather via selection of stable collaterally sensitive clones. Thus, our work suggests strategies for rationalizing drug (or drug combination) design beyond the focus on traditional terminal stages of clonal evolution and emphasizes an understanding of the underlying evolutionary trajectories and intermediate stages to fully exploit tumor vulnerabilities.

RESULTS

Drugs with particular fitness landscapes can affect clonal intermediates and diversify subpopulation trajectories

To explore the conceptual idea of temporal collateral drug sensitivity arising from tumor subpopulation dynamic evolution, we first developed a minimal stochastic branching process mathematical model to examine the effects of distinct predefined fitness landscapes on clonal evolution (see Methods and Supplemental Methods for details).

Under the premise of a step-wise clonal evolution, we assumed a fitness landscape built based on multivariate Gaussian distributions with an intermediate and terminal stage (Fig 1A). In the presence of drug, the simulation revealed the treatment-naïve initial population would expectably evolve toward higher fitness (Supp Fig S1A and S1E). We next hypothesized the existence of an evolutionary trade-off at the intermediate stage of clonal evolution – specifically exhibiting a suboptimal fitness to another drug D (Fig 1D). As such, during a clonal evolution under drug A selection, there exists a treatment window (‘temporary collateral sensitivity’) during which a switch to drug D will lead to a lower fitness of the resulting population (Supp Fig S1B).

Using this same model, we asked what the consequences would be if we first use drug A for resistance selection, followed by drug D – to exploit this temporal collateral sensitivity. Simulation results suggest that sequential drug switch and selection can change the propensities of clonal evolution, and lead to divergent trajectories (Supp Fig S1C and S1F). Specifically, continued selection in drug D led to distinct trajectories that although all have high fitness for drug D (Supp Fig S1D), now have populations with diverse fitness to drug A (Supp Fig S1C). Thus, examining drugs with distinct fitness landscapes can potentially expose a treatment window with temporal vulnerabilities during clonal evolution, and the choice of sequential drug selection can change/diversify subsequent clonal trajectories. Of note, the mathematical model was based on our preconception of a step-wise fitness landscape. The model can be modified and/or extended with incorporation of random field models of fitness landscapes (e.g. NK model) and/or examination of different drug schedules. However, here we chose next to turn to an experimental system to screen and validate this conceptual idea more concretely.

A pharmacological screen identifies intermediate BCR-ABL1 V299L populations with collateral sensitivity to crizotinib, foretinib, cabozantinib, and vandetanib

Motivated by the results from the stochastic branching process model, we examined combined pharmacological profiles and *in vitro* drug resistance selection in a murine preclinical model of Ph+ acute lymphoblastic leukemia (Boulos et al., 2011; Williams et al., 2007). Ph+ ALL is a particularly relevant and tractable model – in contrast to chronic myeloid leukemia (CML), Ph+ ALL is an aggressive disease and has rapid relapse following treatment with frequent selection of BCR-ABL1 kinase domain mutations (Ottmann and Pfeifer, 2009; Soverini et al., 2006). Here, we derived resistant cell lines with dose escalating concentrations of BCR-ABL1 inhibitors (Fig 2A). Each derived cell line (totaling close to 180 cell lines) was screened across a diverse set of small molecule inhibitors. In our preliminary screen, through several independent dasatinib selections, we observed initial resistance to dasatinib and cross-resistance to bosutinib (Fig 2B). Strikingly, we also observed strong sensitization (i.e. collateral sensitivity) to crizotinib, foretinib, vandetanib, and cabozantinib. These drugs are typically recognized as cMET and/or VEGFR inhibitors, but the sensitization we found did not appear to be generalizable across all such targeted drugs examined – suggesting a mechanism of action beyond these known canonical targets.

We continued with multiple rounds of independent selection to first confirm this was indeed a robust phenotype. With over ten independent selection series, we observed a consistent sensitization to these four small molecules upon the development of cross-resistance to dasatinib and bosutinib. Most interestingly, as the cells continued to evolve toward cross-resistance to imatinib, nilotinib, and at times ponatinib, the magnitude of collateral sensitivity diminished (Fig 2C). This was particularly prominent for crizotinib, foretinib, and cabozantinib. Vandetanib appeared to largely retain its collateral sensitivity over the entirety of clonal evolution. In addition to this sensitization, we also observed other distinct patterns of collateral resistance and sensitivity, even within the same drug through independent selections. This highlights the stochastic nature of this process. As would be the case from Luria and Delbruck's fluctuation analyses, this variability suggests selection of distinct

clones for outgrowth, which would lead to subsequent different phenotypic pharmacological response patterns.

Since on-target ABL1 kinase domain mutations are a common mechanism of resistance to BCR-ABL1 inhibitors, we PCR-amplified and Sanger sequenced the kinase domain of ABL1. We observed a perfect concordance between the collateral sensitivity to crizotinib, foretinib, cabozantinib, and vandetanib, and the presence of a single V299L mutation in ABL1 (Fig 2C and 2D). Remarkably, the dasatinib/bosutinib-resistant cells containing the V299L mutation further evolved to develop V299L compound mutations under continued drug selection. The emergence of V299L compound mutations was coincident with the reduced collateral sensitization (Fig 2C). Although variant calls from RNA-seq of select cell lines containing BCR-ABL1 V299L or V299L compound mutants revealed additional passenger SNVs and indels (Supp Fig S2), the only mutation shared among cell lines with the sensitization phenotype and that went from 0% to 100% variant allele frequency was c. 895G>C, leading to BCR-ABL1 V299L (Supp Fig S3 and Supp Table S1).

To further confirm that BCR-ABL1 V299L is the causative mutation in sensitizing cells to these four small molecules, we performed dose response experiments using isogenic Ba/F3 cell lines. While BCR-ABL1 V299L expectedly conferred resistance to dasatinib and bosutinib, we observed strong and robust sensitization to crizotinib, foretinib, cabozantinib, and vandetanib (Fig 2E).

BCR-ABL1 V299L is pre-existing and selected for during drug treatment

We next investigated whether the BCR-ABL1 V299L and/or V299L compound mutants were pre-existing in the parental population. Since both Sanger sequencing and variant-calls from RNA-seq did not detect BCR-ABL1 V299L in the parental population, the actual estimate would at most exist at a level that is below the detection limit of these technologies (~10% for Sanger sequencing, and 0.1–1% for NGS technologies (Robasky et al., 2014)). Here we developed a stochastic mathematical model based on nonhomogeneous continuous-time multi-type birth-death process (see Methods and Supplemental Methods). The model incorporates the background mutation rate, birth and death rates of the individual subpopulations (derived based on experimentally determined net growth rates), and death rate in the presence of drug (derived from dose response curves). We performed Monte Carlo simulations with various combinations of parameter values, taking into account the uncertainty and initially zero or some non-zero value of BCR-ABL1 V299L or V299L compound mutant subpopulation at the beginning of the simulation. The only set of parameters that best explain our experimentally observed kinetics (9 days for initial outgrowth, and V299L in going from < 0.1% to >99.9% at day 9) is the pre-existence of a BCR-ABL1 V299L subpopulation at 0.0082% in the parental population (Fig 3A- C and Supp Fig S4A and S4B). Furthermore, the model predicts that the BCR-ABL1 V299L compound mutant could exist either at zero or a very minor (i.e. < 0.0006%) percentage at the beginning of the selection experiments (Fig 3D and Supp Fig S4A and S4B). In addition, our sensitivity analysis demonstrates that this result is robust and largely independent of background mutation rates and birth/death rates (Fig 3E). The major determinant of the kinetics and fractional appearances of subclones is the initial subpopulation size.

Using the estimated pre-existing fractions of BCR-ABL1 V299L and V299L compound subpopulations, we next determined the approximate treatment window for exploiting collateral sensitivity, which was driven by the predominance of V299L single mutation at intermediate stages of clonal evolution. We performed mathematical modeling based on a system of ordinary differential equations to fully simulate our selection experiments – with automatic dose escalation upon outgrowth (Fig 3F and 3G). The model revealed an approximate range of 1 to 3 weeks where BCR-ABL1 V299L was the dominating subpopulation fraction and, as such, conferring a persistent sensitization to drugs such as foretinib (Fig. 3H and 3I).

Another aspect with regards to timing and clinical management is the scheduling of drug combinations. To examine this question, we simulated tumor kinetics under different drug schedules (single, concurrent, or alternating of dasatinib and foretinib). We observed that when the pre-existing V299L subpopulation is small, the most synergistic combination was that of an alternating regimen, especially if the concurrent treatment requires dose reduction (Supp Fig S4C). Here foretinib would be effective only after the enrichment of the V299L subpopulation following dasatinib treatment. However, once V299L reached a substantial fraction, the therapeutic benefit of an alternating treatment is limited as we risk the outgrowth of the BCR-ABL1 WT subpopulation during the foretinib cycle, or the outgrowth of V299L compound from V299L subpopulations during the dasatinib cycle (Supp Fig S4D). As such, the efficacious strategy remains to be a concurrent treatment of dasatinib and foretinib, or alternating treatments of a duration that can control the outgrowth of the BCR-ABL1 WT and V299L effectively.

BCR-ABL1 V299L confers collateral sensitivity through an on-target BCR-ABL1 inhibition

Our demonstrated efficacy in isogenic Ba/F3 cell lines suggest that the collateral sensitivity is likely to act through an on-target BCR-ABL1 inhibition. To confirm, we made various phenotypic and signaling measurements. BCR-ABL1 promotes cell cycle entry (G1-to-S phase transition) and its inhibition results in G1 cell cycle arrest (Andreu et al., 2005; Cortez et al., 1997). As such we posited that a similar cell cycle profile would provide, albeit a downstream read-out, evidence of potential on-target ABL1 inhibition. Therefore, we examined cell cycle profiles of BCR-ABL1 WT and BCR-ABL1 V299L cells upon drug treatment. As expected, we observed an induction of G1 arrest in both WT and V299L cell lines upon treatment with BCR-ABL1 inhibitors (Fig 4A). In addition, as was expected from previous dose response curves, higher concentrations of dasatinib and bosutinib were required for G1 arrest in the presence of V299L. However, lower concentrations of vandetanib, cabozantinib, crizotinib, and foretinib was sufficient to induce a G1 arrest in BCR-ABL1 V299L cells (Fig 4A). Furthermore, crizotinib and foretinib appeared to exhibit off-targets at high concentrations, leading to a prominent G2/M arrest in both BCR-ABL1 WT and V299L cell lines. This was consistent with a previous report of G2/M arrest (and mitotic catastrophe) induced by foretinib in CML K562 cells (Dufies et al., 2011), albeit the exact mechanism mediating this effect remains unknown.

Since Stat5 is a substrate of BCR-ABL1 and a surrogate biomarker of BCR-ABL1 activity (O'Hare et al., 2012), we also examined phospho-Stat5 levels and cleaved PARP, as a marker

for apoptosis via flow cytometry. As expected, we observed down-regulation of pStat5 upon treatment with BCR-ABL1 inhibitors, and again with a higher required concentration for dasatinib/bosutinib in V299L cell lines (Fig 4B and Supp Fig S5). Although we observed no down-regulation of pStat5 in BCR-ABL1 WT cell lines upon treatment with vandetanib, cabozantinib, crizotinib, and foretinib, the occurrence of down-regulation in pStat5 in V299L cell lines suggests an on-target ABL1 inhibition in the presence of BCR-ABL1 V299L. An increased cPARP level without a strong pStat5 inhibition at high concentrations of crizotinib and foretinib in both BCR-ABL1 WT and V299L cell lines is consistent with the earlier cell cycle profiles suggesting an off-target mechanism of action at the higher doses.

To show direct inhibition of ABL1, we further performed *in vitro* kinase assays with purified recombinant active ABL1 WT and ABL1 V299L mutant. We observed preferential inhibition of kinase activity for V299L mutant compared to WT for the four small molecules – crizotinib, foretinib, cabozantinib, and vandetanib (Fig 4C and Supp Fig S6A). Given the particularly large fold change in preferential inhibition for vandetanib against ABL1 V299L based on our kinase and viability assays, we also performed computational docking studies. Intriguingly, bosutinib and vandetanib share close chemical structures: quinoline (for bosutinib) or quinazoline (for vandetanib) group for occupying the adenine pocket, a substituted aniline group for occupying the hydrophobic pocket, and a long-chain extended into the solvent region for increased solubility (Supp Fig S6B). Our docking results support this insight, with vandetanib binding to ABL1 WT and V299L in a similar conformation to that for bosutinib (Fig 4D and 4E). BCR-ABL1 inhibitor bosutinib forms a hydrogen bond to the hinge region of ABL1 (a feature shared by most kinase inhibitors), and via its nitrile group van der Waals contacts with T315 and V299 and water-mediated hydrogen bond network to the DFG motif (Levinson and Boxer, 2012, 2014). Mutation V299L results in steric hindrance to the nitrile group, and the likely cause of clinically observed resistance. Most notably, docking of vandetanib to V299L kinase domain suggests leucine capable of making an additional non-polar contact with vandetanib (Fig 4E and Supp Fig S6C). Energetic calculations suggest vandetanib in complex with V299L mutant is stabilized by approximately ten fold through improved packing – primarily via interaction between V299L and the quinazoline group of vandetanib.

To rule out any off-target effects, we examined RNA-seq differential expression of our parental, V299L-, and V299L compound-containing cell lines. Unsupervised hierarchical clustering showed the expected groupings with respect to the cell lines' ABL1 mutational status (Supp Fig S7A). Although there were limited differentially expressed genes among the cell lines (Supp Fig S7B), gene set enrichment analyses did not reveal any statistically significant phenotypic or functional categories. This suggests that V299L (and V299L compounds) does not affect cellular state. Next, we assessed the possibility that this mutant would lead to substrate specificity changes downstream BCR-ABL1. We integrated results from a recently-developed algorithm named KINspect (Creixell et al., 2015) that identifies those residues most and least likely to contribute to substrate specificity by exploring millions of different specificity models. The algorithm confirmed that V299L, with a KINspect specificity score of 0.05, is unlikely to disrupt or significantly change substrate

specificity (Supp Table S2). Taken together, these data indicate that the collateral sensitization conferred by BCR-ABL1 V299L is due to on-target ABL1 inhibition.

Collaterally sensitive drugs against BCR-ABL1 V299L exhibit in vivo efficacy

To investigate whether the collateral sensitivity translates to *in vivo* efficacy, we tail-vein injected BCR-ABL1 WT or V299L cell lines into immunocompetent syngeneic recipient mice. Upon the cytological appearance of an initial tumor burden on day 10 post transplantation, we treated mice once daily with vehicle, imatinib, dasatinib, foretinib, or vandetanib. We first assessed the overall tumor burden using whole-mouse bioluminescence imaging pre- and post-treatment. As expected, we observed a reduction in tumor burden upon treatment with imatinib and dasatinib in mice with WT BCR-ABL1 (Fig 5A and 5B). Foretinib and vandetanib had modest to no *in vivo* efficacy. However, in mice with BCR-ABL1 V299L, imatinib and dasatinib exhibited no antitumor responses, while treatment with foretinib or vandetanib led to a significant 3-log fold reduction in tumor burden compared to vehicle control (Fig 5B).

Animals transplanted with these Ph+ ALL cells also develop splenomegaly. Whereas treatment of WT BCR-ABL1 ALL-bearing mice with foretinib or vandetanib did not lead to any reduction in spleen size, mice bearing BCR-ABL1 V299L ALL exhibited a 3- to 4-fold reduction in spleen size upon treatment (Fig 5C and 5D). Of note, we observed a moderate fitness defect for BCR-ABL1 V299L cells relative to cells expressing WT BCR-ABL1. This was apparent both based on *in vitro* growth assays and in the disease onset for these tumors. As such, BCR-ABL1 WT mice were also sacrificed a few days early for imaging and assessment of spleen size. BCR-ABL1 mutants have been known to exhibit different fitness in the absence of drug, which may be due in part to moderate catalytic inefficiencies and/or downstream substrate specificity (Griswold et al., 2006; Skaggs et al., 2006).

We next evaluated the overall survival of treated animals. We performed once daily oral gavage of vehicle, imatinib, dasatinib, foretinib, or vandetanib for one week starting at day 10 post-transplantation with cells expressing either BCR-ABL1 WT or V299L. In mice with WT BCR-ABL1, we observed an increase in median survival of 4 and 5 days upon treatment with imatinib or dasatinib, respectively (Fig 5E, $P < 0.001$). Treatments with foretinib or vandetanib did not lead to a statistically significant increase in survival for mice bearing WT BCR-ABL1. In contrast, we observed a significant extension in median survival of 3 to 4 weeks when mice with BCR-ABL1 V299L were treated with foretinib or vandetanib. Most notably, a subset of the animals in these cohorts achieved long-term survival without relapse.

Sequential drug combination selection reveals divergent clonal trajectories

Given the relevance of collateral sensitivity to treatment response in this model, we next wondered how the choice of sequential drug selection affects the occurrence of temporal collateral sensitivity and clonal trajectories. To examine these questions, we performed a similar drug resistance selection experiment as before. However, as opposed to using a single drug at dose escalating concentrations, we treated cells with a single dose of drug A at an IC90 concentration, followed, after initial tumor cell regrowth, by a switch to drug B at dose escalating concentrations (Fig 6A).

Here, we again observed that, upon selection with dasatinib or bosutinib, the parental ALL cell line has a propensity toward the development of BCR-ABL1 V299L mutations (Fig 6B). A single round of selection with the other non-ABL1 targeting small molecules led to zero or one mutations in the ABL1 kinase domain. In either case, the resulting pharmacological response revealed no pronounced phenotypes of collateral resistance or sensitivity.

Continued selection with BCR-ABL1 V299L ALL cells using dose-escalating concentrations of non-ABL1 targeting small molecules led to continued evolution toward V299L compound mutants. In some cases, the V299L compound (i.e. V299L/F317L) resulted in pronounced attenuation of collateral sensitivity, whereas in others (e.g. V299L/D276G or V299L/Q252H), the collateral sensitivity appeared to be retained (Fig 6C). Structural modeling and analysis shows that F317L independently weakens vandetanib binding through diminished packing interactions with the quinazoline group. In contrast, changes in Q252 and D276 are expected to have minimal effect – the former is solvent exposed and makes only weak intra-protein interactions and the latter is over 20 Å away from the active site. Together, these data suggest additional mutations in ABL1 can result in neutral or disruption of the stabilization previously created via V299L.

We next examined the effect of initial selection with the collaterally sensitive small molecules, followed by dose escalating selection with dasatinib. We observed that BCR-ABL1 V299L was no longer the dominating resistant population at outgrowth. Although all the mutations continue to be localized to the ABL1 kinase domain, we observed a more diverse set of trajectories, including BCR-ABL1 T315I (Fig 6C). Thus, the order in which cells are exposed to drugs/develop resistance can affect the propensities of cells toward specific resistance mechanisms. In particular, we still do observe V299L in these sequential selection experiments; however, this pre-selection of e.g. foretinib followed by dasatinib potentially diminished the pre-existing predominant V299L subpopulation and enabled the stochastic selection and outgrowth of other subclones.

Small molecule screen reveals compounds with diverse fitness landscapes across clonal evolution

We have thus far examined collateral sensitivity and resistance using a limited set of targeted and chemotherapeutics. We next wanted to investigate the diversity of fitness landscapes in a broader small molecule space. Capitalizing on the known trajectories of our parental ALL cell line in evolving toward V299L and subsequently V299L compound mutants upon dasatinib selection, we performed a small molecule screen of 391 compounds against the parental, BCR-ABL1 V299L, and V299L/E255K cell lines (corresponding to the initial, intermediate and terminal stage of clonal evolution) (Fig 7A).

We can schematically visualize the EC50s as they are mapped onto a fitness landscape, consisting of these three clonal stages. Of the positive controls, there are molecules such as bosutinib (Fig 7B) and imatinib (Fig 7C) where there is an escalating fitness with progressive stages of clonal evolution. In contrast, there are other drugs such as vandetanib and foretinib where intermediate and/or terminal stages consist of valleys instead of peaks in the fitness landscape – an illustration of collateral sensitivity. The other possibility is a valley for the intermediate and a peak for the terminal, as was observed for axitinib (Fig 7F) and

crizotinib (Fig 7G). Interestingly, axitinib was recently reported to exhibit efficacy against BCR-ABL1 T315I (as well as V299L), through an on-target ABL1 inhibition (Pemovska et al., 2015). Studies here suggest that the V299L/E255K compound abrogates such efficacy for axitinib. These are among several small molecules that appeared to exhibit these distinct fitness landscapes, with effects ranging from persistent to temporal collateral resistance or sensitivity.

DISCUSSION

Our view of tumor clonal evolution as a dynamic process led us to propose the existence of additional vulnerabilities and evolutionary tradeoffs for exploitation – en route toward terminal drug resistance. Notably, using combined *in vitro* drug resistance selection and pharmacological profile experiments, we have uncovered a temporal collateral sensitivity phenomenon using a preclinical murine model of Ph+ ALL. Sequencing analysis in partnership with kinetic mathematical modeling revealed that this was driven by a selection of a pre-existing BCR-ABL1 V299L and subsequently BCR-ABL1 V299L compounds-containing stable clonal subpopulations. As such, this is quite distinct from temporal network rewiring mechanisms of drug synergy/sensitization. Our RNA-seq, phenotypic, signaling, binding, and docking analyses indicate that the sensitization to non-classical BCR-ABL1 inhibitors crizotinib, foretinib, vandetanib, and cabozantinib was driven by an on-target ABL1 inhibition in the presence of the V299L mutation. Clinically, V299L mutations have been observed in CML and Ph+ ALL patients, and occurs upon dasatinib or bosutinib treatment failure (at 5–7%) (Jabbour et al., 2012; Ravandi et al., 2010). V299L compound mutations are also clinically observed following sequential BCR-ABL1 TKI treatments (Zabriskie et al., 2014), and in one study of CML patients, V299L was the second most common component of compound mutations (at 20%) (Khorashad et al., 2013).

The mechanism of action for this collateral sensitivity was surprising: a gained on-target ABL1 inhibition realized by new interaction forged through the initial ABL1 mutation. The selectivity toward a specific kinase mutant vis-à-vis WT is not unprecedented. Recently axitinib has been shown to be active against BCR-ABL1 T315I (and other BCR-ABL1 mutants, including V299L) (Pemovska et al., 2015). Here axitinib binds to the active site of ABL1 in a distinct conformation different from its known target VEGFR2. In contrast, pan-Aurora inhibitor danusertib binds to ABL1 T315I in similar conformation, with Ile315 mimicking Leu210 in Aurora A (Modugno et al., 2007). Our findings and these studies suggest existing compounds may exhibit selectivity toward kinase mutants over WT that in some cases due to the mutation changing to an ‘on-target mimetic’. This highlights opportunities for potential experimental and *in silico* screens of existing small molecules for mutant selectivity and possibly provide alternatives to existing drugs with known adverse side effects (e.g. ponatinib and nilotinib with vascular occlusive events (Valent et al., 2015)).

Capturing the time window for temporal collateral sensitivity can be challenging. However, for Ph+ ALL or CML, biopsies and quantitative analysis of BCR-ABL1 transcript levels are routinely utilized for monitoring disease progression. This provides the opportunity to strategize the timing for incorporation of non-classical BCR-ABL1 inhibitors for patients. In solid tumors and other hematopoietic cancers, utility of circulating tumor cells or DNA

(albeit at limited resolution) may be used as additional modalities. Nevertheless, challenges remain for the identification and improved sensitivity of biomarker identification.

Ultimately, optimal clinical management will also require the incorporation and consideration of current standard of care. In the case for Ph+ ALL, current regimens include fractionated chemotherapy combinations, such as Hyper-CVAD with addition of a BCR-ABL1 inhibitor, and most often followed by stem cell transplantation. However, incorporation of TKIs into chemotherapy regimens has not dramatically improved remission duration (Ottmann and Pfeifer, 2009), suggesting a need for additional understanding on the effects of chemotherapy and TKIs and/or clinical management for this aggressive disease.

Our modeling presented here provides a conceptual understanding of temporal collateral sensitivity and estimations of pre-existing populations. Additional experimental and mathematical modeling will be useful to examine different drug scheduling strategies. For example, alternating treatment may be of value if cycling between classical BCR-ABL1 inhibitors and collaterally sensitive drugs may impede the continual evolution toward compound mutants. However, if a large wild-type fraction still persists after the initial log fold tumor reduction, a more practical strategy would involve concurrent treatments with inclusion of classical BCR-ABL1 inhibitors (or hyper-fractionation of the alternating regimen) for the effective management of disease. Mathematical modeling of these scenarios along with incorporation of various factors (e.g. pharmacokinetics, clonal interference/cooperation, microenvironments, etc.) and applications from control theory (Swan, 1990) and adaptive drug design (Gatenby et al., 2009) will inform scheduling implications in the context of temporal and/or persistent collateral sensitivity trade-offs.

Undoubtedly different parental cell lines and patients prior to diagnosis will exhibit different propensities toward resistance. This study reveals that there can potentially be a treatment window to exploit temporal collateral sensitivity at predictable clonal evolutionary trajectories. Furthermore, this work highlights an approach for combining extensive drug resistance selection experiments with pharmacological profiles to identify novel vulnerabilities during the course of tumor clonal evolution. In particular, this approach has broad applications for studies beyond tyrosine kinase inhibitors. For instance, multiple rounds of chemotherapy selection can result in distinct step-wise progression via multiple mutations. The pharmacological profiles would not only identify these functional clonal evolutionary states that would otherwise be difficult solely based on genome sequencing, but also the identification of specific vulnerabilities at such stages. It is worth noting that this mechanism does not have to be restricted to on-target mutations, but is also a potential consequence of dysregulation in compensatory pathways. Our Ph+ ALL model exhibits strong evolutionary constraints toward on-target point mutations as mechanism of resistance. Different cancer types and drug classes (including chemotherapy) will undoubtedly have distinct mechanisms. Nevertheless, similarity in evolutionary constraints – including prevalence of on-target kinase domain mutations in ALK (in non-small-cell lung cancer) or cKIT (in gastrointestinal stromal tumor) and known compensatory pathways (e.g. in EGFR, IGFR1, cMET, etc) presents opportunities to survey more densely their clonal evolutionary trajectories and potential intermittent vulnerabilities.

EXPERIMENTAL AND COMPUTATIONAL PROCEDURES

Cell lines and chemicals

Murine derived Ph+ALL cell line containing BCR-ABL1 p185 (Williams et al., 2006, 2007) was cultured in RPMI medium supplemented with 10% FBS, 4 mM L-glutamine, 5 μM β-mercaptoethanol. The murine Ba/F3 parental cell line, received from the Druker lab, cultured in RPMI medium supplemented with 10% FBS and 10 ng/mL recombinant murine IL3 (R&D Systems). Mutant Ba/F3 expressing BCR-ABL1 wild-type or BCR-ABL1 V299L were generated as previously described (Shah et al., 2002). Mutant Ba/F3 were cultured in RPMI medium supplemented with 10% FBS. All cell lines were tested and shown to be free of *Mycoplasma* using PCR-based (ATCC) and biochemical-based (Lonza) methods. All drugs were obtained from LC Laboratories or Selleck Chemicals.

Drug resistance selection

Cells were plated at 0.5 million cells/mL and treated at desired drug concentrations. Cells were monitored each day. Upon outgrowth (i.e. cell density reaching 4–5 million cells/mL), cells were 1) frozen down, 2) allowed to recover in no-drug medium, or 3) plated again at 0.5 million cells/mL and treated at the next drug dose. For cells in drug-selection condition, medium was changed every week. For cells recovering in no-drug medium, genomic DNA was extracted for PCR amplification and Sanger sequencing of the ABL1 kinase domain, and dose responses were performed. The stability of the cell line in no-drug medium was confirmed through both Sanger sequencing and dose responses, performed periodically up to 2 months post-recovery.

Statistical analyses

Statistical analyses were performed using Prism v5 (GraphPad) and R v3.2.0. Comparisons in tumor burden reduction were assessed using Mann-Whitney test. RNA-seq differential expression analyses were performed using DEseq package in R. Survival of mice was analyzed with Kaplan-Meier method with significance assessed using log-rank test.

Supplementary Material

Refer to Web version on PubMed Central for supplementary material.

Acknowledgments

We thank Peter Bruno and Christian Braun for critical review and feedback on this manuscript, and Stuart Levine and Jie Wu from the MIT BioMicroCenter and Glen Paradis from the Koch Institute Flow Cytometry Core for services and advices. This work was supported by the Koch Institute Support (core) Grant P30-CA14051 from the National Cancer Institute, the Integrative Cancer Biology Program Grant U54-CA112967 (to M.T.H., D.A.L., and B.T.), the National Institutes of General Medical Sciences GM082209 (to B.T), the Ludwig Foundation (to M.T.H.) and the Go Mitch Go Foundation (to M.T.H.). B.Z. and R.S. are supported by the NIH/NIGMS Interdepartmental Biotechnology Training Program 5T32GM008334. B.Z. is also supported by the National Science Foundation Research Fellowship under Grant No. 1122374. P.C. is supported by postdoctoral fellowships of the Ludwig Fund and Helen Hay Whitney Foundation. B.Z. is a consultant for ARIAD Pharmaceuticals, Inc. J.R.P. is an employee and shareholder of ARIAD Pharmaceuticals, Inc. D.A.L. is a consultant/advisory board member of Merrimack Pharmaceuticals, Genentech, and Complete Genomics. Remaining authors declare no potential conflict of interests.

References

Andersson DI, Hughes D. Antibiotic resistance and its cost: is it possible to reverse resistance? Nat Rev Microbiol. 2010; 8:260–271. [PubMed: 20208551]

Andreu EJ, Lledó E, Poch E, Ivorra C, Albero MP, Martínez-Climent JA, Montiel-Duarte C, Rifón J, Pérez-Calvo J, Arbona C, et al. BCR-ABL induces the expression of Skp2 through the PI3K pathway to promote p27Kip1 degradation and proliferation of chronic myelogenous leukemia cells. Cancer Res. 2005; 65:3264–3272. [PubMed: 15833859]

Bhang HC, Ruddy Da, Krishnamurthy Radhakrishna V, Caushi JX, Zhao R, Hims MM, Singh AP, Kao I, Rakiec D, Shaw P, et al. Studying clonal dynamics in response to cancer therapy using high-complexity barcoding. Nat Med. 2015

Boulos N, Mulder HL, Calabrese CR, Morrison JB, Rehg JE, Relling MV, Sherr CJ, Williams RT. Chemotherapeutic agents circumvent emergence of dasatinib-resistant BCR-ABL kinase mutations in a precise mouse model of Philadelphia chromosome-positive acute lymphoblastic leukemia. Blood. 2011; 117:3585–3595. [PubMed: 21263154]

Chen G, Mulla WA, Kucharavy A, Tsai HJ, Rubinstein B, Conkright J, McCroskey S, Bradford WD, Weems L, Haug JS, et al. Targeting the Adaptability of Heterogeneous Aneuploids. Cell. 2015; 160:771–784. [PubMed: 25679766]

Cortez D, Reuther G, Pendergast aM. The Bcr-Abl tyrosine kinase activates mitogenic signaling pathways and stimulates G1-to-S phase transition in hematopoietic cells. Oncogene. 1997; 15:2333–2342. [PubMed: 9393877]

Creixell P, Palmeri A, Miller CJ, Lou HJ, Santini CC, Nielsen M, Turk BE, Linding R. Unmasking Determinants of Specificity in the Human Kinome. Cell. 2015; 163:187–201. [PubMed: 26388442]

Ding L, Ley TJ, Larson DE, Miller Ca, Koboldt DC, Welch JS, Ritchey JK, Young Ma, Lamprecht T, McLellan MD, et al. Clonal evolution in relapsed acute myeloid leukaemia revealed by whole-genome sequencing. Nature. 2012; 481:506–510. [PubMed: 22237025]

Dufies M, Jacquel A, Robert G, Cluzeau T, Puissant A, Fenouille N, Legros L, Raynaud S, Cassuto J, Luciano F, et al. Mechanism of action of the multikinase inhibitor Foretinib. Cell Cycle. 2011; 10:4138–4148. [PubMed: 22101270]

Fisher R, Pusztai L, Swanton C. Cancer heterogeneity: implications for targeted therapeutics. Br J Cancer. 2013:1–7.

Gatenby RA, Silva AS, Gillies RJ, Frieden BR. Adaptive therapy. Cancer Res. 2009; 69:4894–4903. [PubMed: 19487300]

Gerlinger M, Rowan AJ, Horswell S, Larkin J, Endesfelder D, Gronroos E, Martinez P, Matthews N, Stewart A, Tarpey P, et al. Intratumor heterogeneity and branched evolution revealed by multiregion sequencing. N Engl J Med. 2012; 366:883–892. [PubMed: 22397650]

Griswold IJ, MacPartlin M, Bumm T, Goss VL, O'Hare T, Lee Ka, Corbin AS, Stoffregen EP, Smith C, Johnson K, et al. Kinase domain mutants of Bcr-Abl exhibit altered transformation potency, kinase activity, and substrate utilization, irrespective of sensitivity to imatinib. Mol Cell Biol. 2006; 26:6082–6093. [PubMed: 16880519]

Hill JA, O'Meara TR, Cowen LE. Fitness Trade-Offs Associated with the Evolution of Resistance to Antifungal Drug Combinations. Cell Rep. 2015; 10:809–819.

Imamovic L, Sommer MOA. Use of collateral sensitivity networks to design drug cycling protocols that avoid resistance development. Sci Transl Med. 2013; 5:204ra132.

Jabbour E, Morris V, Kantarjian H, Yin CC, Burton E, Cortes J. Characteristics and outcomes of patients with V299L BCR-ABL kinase domain mutation after therapy with tyrosine kinase inhibitors. Blood. 2012; 120:3382–3383. [PubMed: 23086624]

Jensen PB, Holm B, Sorensen M, Christensen IJ, Sehested M. In vitro cross-resistance and collateral sensitivity in seven resistant small-cell lung cancer cell lines: preclinical identification of suitable drug partners to taxotere, taxol, topotecan and gemcitabin. Br J Cancer. 1997; 75:869–877. [PubMed: 9062409]

Khorashad JS, Kelley TW, Szankasi P, Mason CC, Soverini S, Adrian LT, Eide Ca, Zabriskie MS, Lange T, Estrada JC, et al. BCR-ABL1 compound mutations in tyrosine kinase inhibitor-resistant CML: Frequency and clonal relationships. Blood. 2013; 121:489– 498. [PubMed: 23223358]

Kim S, Lieberman TD, Kishony R. Alternating antibiotic treatments constrain evolutionary paths to multidrug resistance. Proc Natl Acad Sci. 2014; 111:14494–14499. [PubMed: 25246554]

Lázár V, Nagy I, Spohn R, Csörg B, Györkei Á, Nyerges Á, Horváth B, Vörös A, Busa-Fekete R, Hrtyan M, et al. Genome-wide analysis captures the determinants of the antibiotic cross-resistance interaction network. Nat Commun. 2014; 5

Levinson NM, Boxer SG. Structural and spectroscopic analysis of the kinase inhibitor bosutinib and an isomer of bosutinib binding to the Abl tyrosine kinase domain. PLoS One. 2012; 7

Levinson NM, Boxer SG. A conserved water-mediated hydrogen bond network defines bosutinib's kinase selectivity. Nat Chem Biol. 2014; 10:127–132. [PubMed: 24292070]

Misale S, Yaeger R, Hobor S, Scala E, Janakiraman M, Liska D, Valtorta E, Schiavo R, Buscarino M, Siravegna G, et al. Emergence of KRAS mutations and acquired resistance to anti-EGFR therapy in colorectal cancer. Nature. 2012; 486:532–536. [PubMed: 22722830]

Modugno M, Casale E, Soncini C, Rosettani P, Colombo R, Lupi R, Rusconi L, Fancelli D, Carpinelli P, Cameron AD, et al. Crystal structure of the T315I Abl mutant in complex with the Aurora kinases inhibitor PHA-739358. Cancer Res. 2007; 67:7987–7990. [PubMed: 17804707]

O'Hare T, Zabriskie MS, Eiring AM, Deininger MW. Pushing the limits of targeted therapy in chronic myeloid leukaemia. Nat Rev Cancer. 2012; 12:513–526. [PubMed: 22825216]

Ottmann OG, Pfeifer H. Management of Philadelphia chromosome-positive acute lymphoblastic leukemia (Ph+ ALL). Hematology Am Soc Hematol Educ Program. 2009:371–381. [PubMed: 20008223]

Pemovska T, Johnson E, Kontro M, Repasky Ga, Chen J, Wells P, Cronin CN, McTigue M, Kallioniemi O, Porkka K, et al. Axitinib effectively inhibits BCR-ABL1(T315I) with a distinct binding conformation. Nature. 2015; 519:102–105. [PubMed: 25686603]

Ravandi F, Brien SO, Thomas D, Faderl S, Jones D, Garris R, Dara S, Jorgensen J, Kebriaei P, Champlin R, et al. First report of phase 2 study of dasatinib with hyper-CVAD for the frontline treatment of patients with Philadelphia chromosome – positive (Ph +) acute lymphoblastic leukemia. Hematology. 2010; 116:2070–2077.

Rickardson L, Fryknäs M, Haglund C, Lövborg H, Nygren P, Gustafsson MG, Isaksson A, Larsson R. Screening of an annotated compound library for drug activity in a resistant myeloma cell line. Cancer Chemother Pharmacol. 2006; 58:749–758. [PubMed: 16528529]

Robasky K, Lewis NE, Church GM. The role of replicates for error mitigation in next-generation sequencing. Nat Rev Genet. 2014; 15:56–62. [PubMed: 24322726]

Shah NP, Nicoll JM, Nagar B, Gorre ME, Paquette RL, Kuriyan J, Sawyers CL. Multiple BCR-ABL kinase domain mutations confer polyclonal resistance to the tyrosine kinase inhibitor imatinib (STI571) in chronic phase and blast crisis chronic myeloid leukemia. Cancer Cell. 2002; 2:117–125. [PubMed: 12204532]

Skaggs BJ, Gorre ME, Ryvkin A, Burgess MR, Xie Y, Han Y, Komisopoulou E, Brown LM, Loo Ja, Landaw EM, et al. Phosphorylation of the ATP-binding loop directs oncogenicity of drug-resistant BCR-ABL mutants. Proc Natl Acad Sci U S A. 2006; 103:19466–19471. [PubMed: 17164333]

Soverini S, Colarossi S, Gnani A, Rosti G, Castagnetti F, Poerio A, Iacobucci I, Amabile M, Abruzzese E, Orlandi E, et al. Contribution of ABL kinase domain mutations to imatinib resistance in different subsets of Philadelphia-positive patients: By the GIMEMA working party on chronic myeloid leukemia. Clin Cancer Res. 2006; 12:7374–7379. [PubMed: 17189410]

Swan GW. Role of optimal control theory in cancer chemotherapy. Math Biosci. 1990; 101:237–284. [PubMed: 2134485]

Valent P, Hadzijusufovic E, Schernthaner G, Wolf D, Rea D, Coutre P. Vascular safety issues in CML patients treated with BCR / ABL1 kinase inhibitors. Blood. 2015; 125:901–906. [PubMed: 25525119]

Williams RT, Roussel MF, Sherr CJ. Arf gene loss enhances oncogenicity and limits imatinib response in mouse models of Bcr-Abl-induced acute lymphoblastic leukemia. Proc Natl Acad Sci U S A. 2006; 103:6688–6693. [PubMed: 16618932]

Williams RT, den Besten W, Sherr CJ. Cytokine-dependent imatinib resistance in mouse BCR-ABL+, Arf-null lymphoblastic leukemia. Genes Dev. 2007; 21:2283–2287. [PubMed: 17761812]

Zabriskie MS, Eide CA, Tantravahi SK, Vellore NA, Estrada J, Nicolini FE, Khoury HJ, Larson RA, Konopleva M, Cortes JE, et al. BCR-ABL1 Compound Mutations Combining Key Kinase Domain Positions Confer Clinical Resistance to Ponatinib in Ph Chromosome-Positive Leukemia. Cancer Cell. 2014:428–442.

Zhao B, Pritchard JR, Lauffenburger DA, Hemann MT. Addressing genetic tumor heterogeneity through computationally predictive combination therapy. Cancer Discov. 2014; 4:166–174. [PubMed: 24318931]

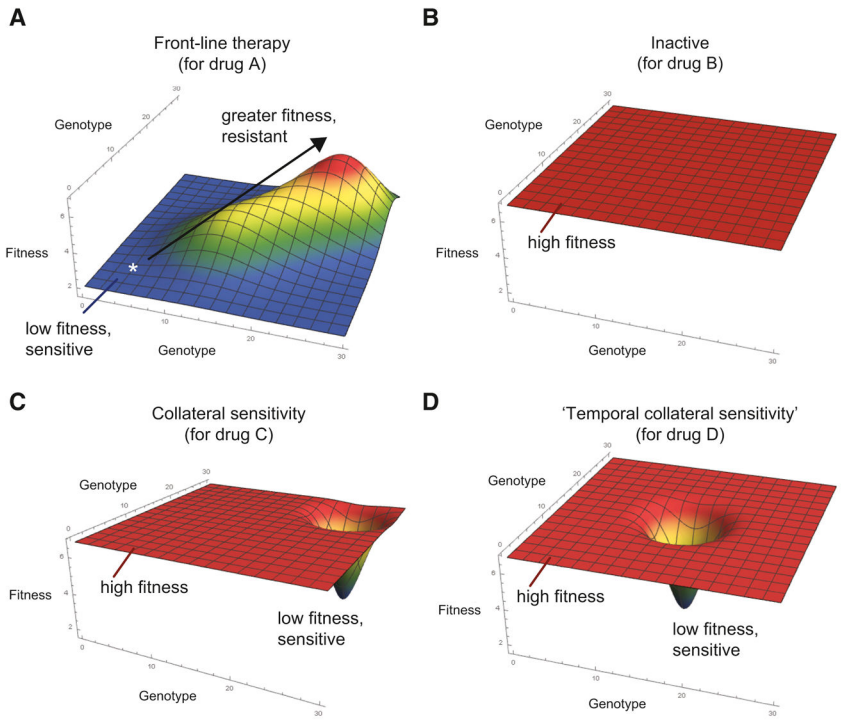

Figure 1. Conceptual fitness landscapes with clonal intermediates

Predefined fitness landscapes can be visualized with a z-axis corresponding to a fitness of the population under a given environmental condition, and x- and y- corresponding to a two-dimensional coordinate of the genotype of each subpopulation. The actual genotype can be in a high-dimensional space, but is explicitly represented here in two-dimensions. The fitness landscape for drug A is composed of two Gaussian peaks for intermediate and terminal stage. In contrast, at the location of the intermediate peak, the corresponding fitness landscape for drug B contains a valley. Initial population is a homogeneous population starting at a low fitness, as indicated by the white asterisk. See also Figure S1.

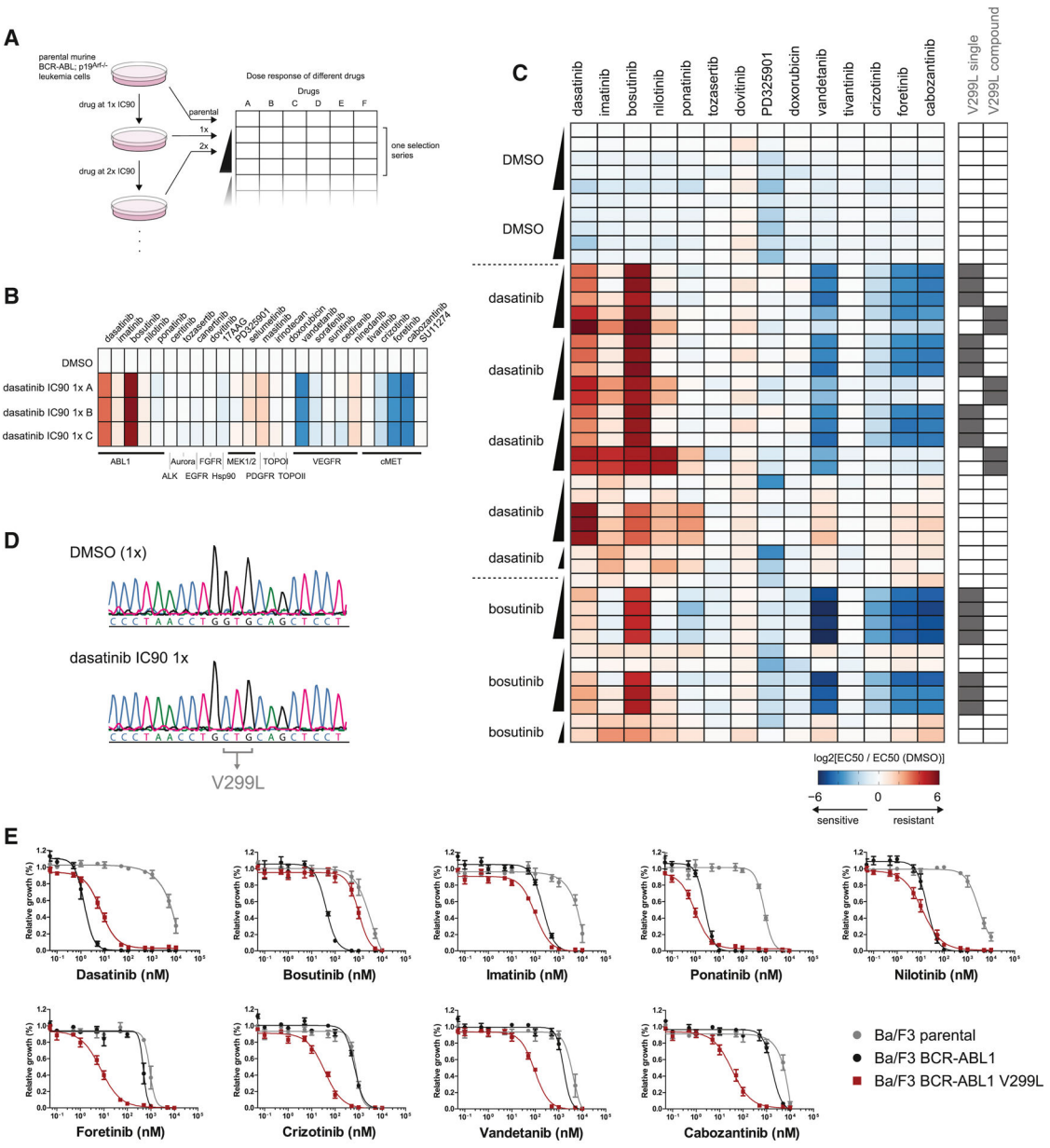

Figure 2. A pharmacological screen of each distinct evolutionary stage to identify persistent and temporal collateral resistance and sensitivity

(A). Schematic of experimental setup for drug resistance selection experiment (see Methods for details). Briefly, a murine derived Ph+ acute lymphoblastic leukemia cell line is treated at IC90 1x drug concentration. Upon recovery and outgrowth, the population is dose escalated to 2x the previous drug concentration. The derived cell line, mimicking a specific stage of the clonal evolution, was allowed to recover and profiled based on viability assays across a panel of targeted and chemotherapeutics. Each selection experiment terminates upon either no outgrowth at the given drug concentration or until IC90 16x. (B) Preliminary drug selection experiment with DMSO control and three independent dasatinib selection at IC90 1x concentration, illustrating collateral sensitivity and resistance. (C) A complete

overview of the drug selection experiments for vehicle, dasatinib, and bosutinib, showing diverse collateral resistance and sensitivity patterns. The black triangles illustrate each independent series of dose escalating concentrations, and hence also an indicator of time. The heatmap shows the log2 transform of the ratio of the EC50s for each drug of given cell line relative to parental cell line. Cell lines with DMSO control grown in parallel had similar EC50s as the parental. The kinase domain of ABL1 was also Sanger sequenced, the subpanel to the right of heatmap illustrates complete concurrence between the sensitization to crizotinib, foretinib, cabozantinib, and vandetanib and single mutational V299L in ABL1. (D) A representative Sanger sequencing of ABL1 V299L. (E) Dose responses of BCR-ABL1 inhibitors and collaterally sensitive inhibitors crizotinib, foretinib, cabozantinib, and vandetanib in Ba/F3 isogenic parental, BCR-ABL1 WT, and BCR-ABL1 V299L cell lines. The sensitization was consistently observed and suggests that V299L is a causative determinant for the sensitization phenotype. See also Figure S2 and S3.

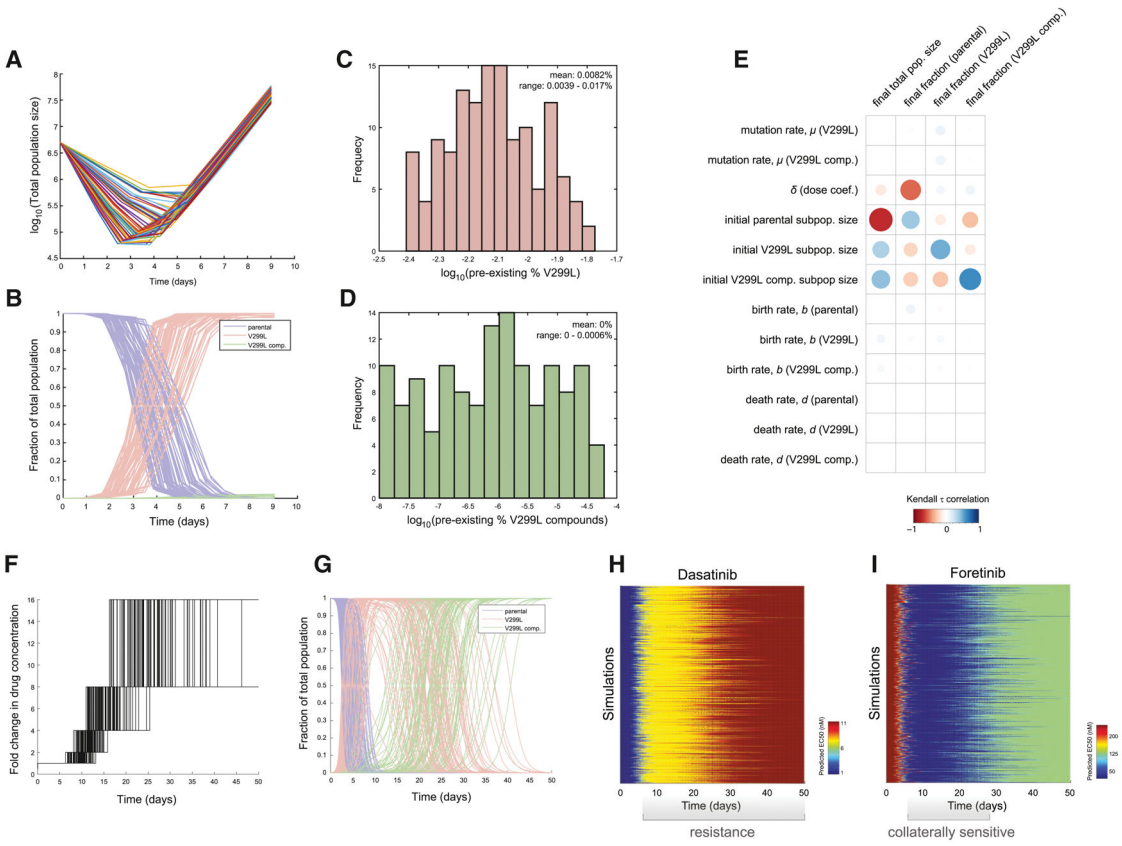

Figure 3. Mathematical models of tumor kinetics predicts pre-existing subpopulations and treatment window

(A–B) Representative stochastic birth/death model simulation results with Monte Carlo sampling of parameters for the first round of selection with dasatinib at IC90 1x concentration. The total population size is shown in (A) and the corresponding subpopulation fractions shown in (B). Simulation results were constrained to those fitting experimental observations (in terms of total population size and tumor composition) at day 0 and 9. Stochastic model predictions at ten evenly distributed time points (connected by line) are shown in plots. (C–D) Distribution of pre-existing subpopulation percentages of BCR-ABL1 V299L (C) and V299L compound (D) for those simulation results that fit our experimental observations. The histogram includes all parameter combinations with at least one simulation run (out of the 50 per parameter combination) that fit the data. The only way to explain our observed kinetics was with the pre-existence of BCR-ABL1 V299L. (E) Sensitivity analyses based on Monte Carlo sampling and stochastic birth/death model showing the effects of each parameter on final tumor population size and tumor composition, as measured by Kendall correlation. Blue and red indicate positive and negative correlation, respectively. The major determinant of final subpopulation sizes was the pre-existing subpopulation sizes. Birth/death rates and background mutation rates had minimal effects. (F–G) Representative ODE simulation kinetics of long-term drug resistance selection with dose escalating concentrations of dasatinib. The dose schedule is shown in (F) and corresponding subpopulation fractions in (G). (H-I) Given the dose escalation simulations, we also predicted the EC50s for the overall population at each time point over

the course of dasatinib selection. This provides an approximate treatment window for which we can observe temporal collateral sensitivity to drugs such as foretinib. The predicted EC50 for the overall population was based on a weighted sum of the known EC50s for individual subpopulations. See also Figure S4.

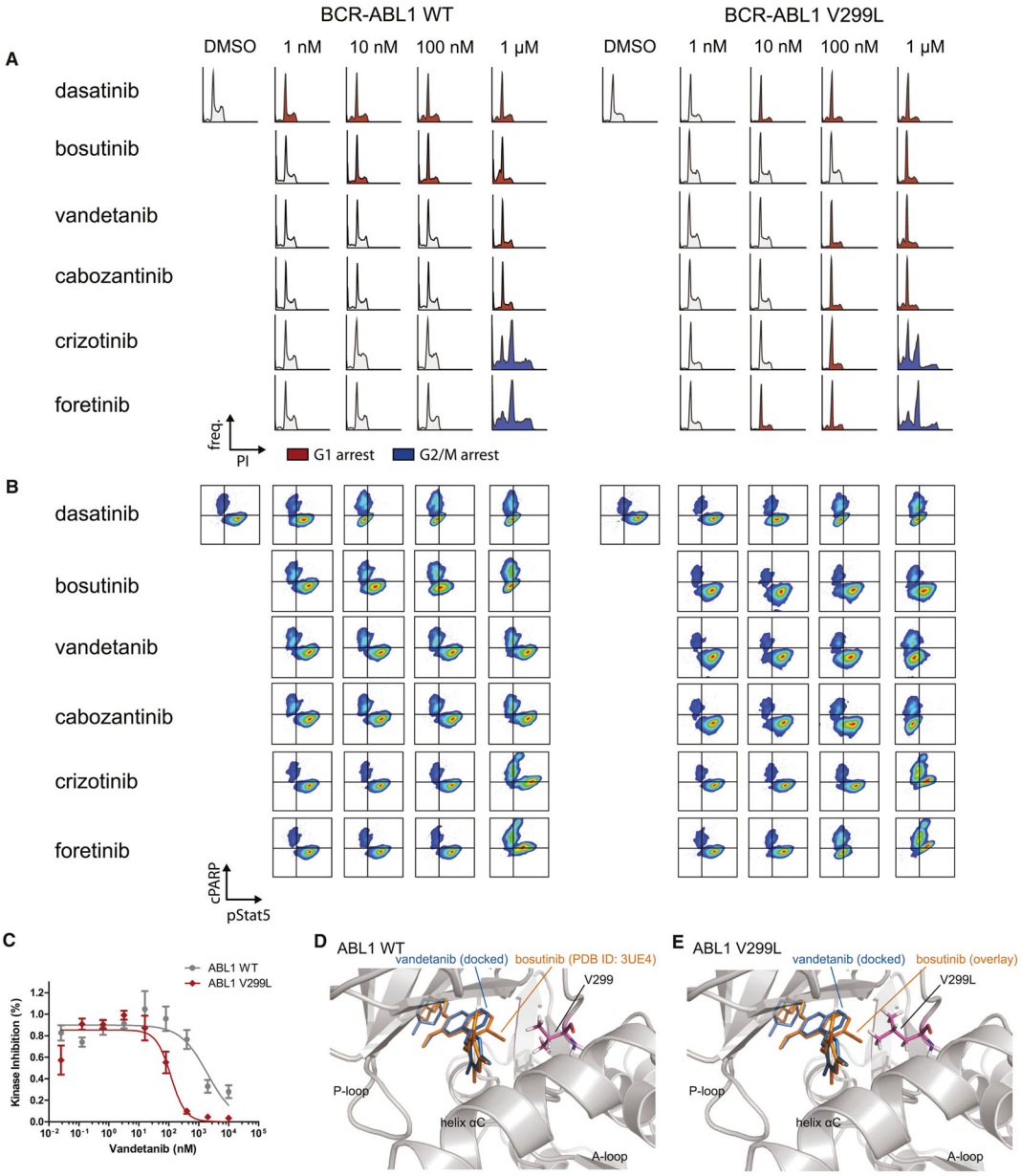

Figure 4. Sensitivity of BCR-ABL1 V299L acts through on-target inhibition of BCR-ABL1

(A). Representative cell cycle profiles taken at 12 hours post treatment *in vitro* for Ph+ ALL cell lines derived from drug selection experiments, either with BCR-ABL1 WT or V299L. Treatments with ABL1 inhibitors led to a G1 arrest, albeit at higher concentrations for V299L cell lines due to resistance. While no G1 arrest was observe upon treatment with crizotinib, foretinib, cabozantinib, and vandetanib in the BCR-ABL1 WT cell line, G1 arrest was observed in the presence of BCR-ABL1 V299L. (B) Representative flow cytometry analysis of phospho-Stat5 (a measure of ABL1 activity) and cleaved-PARP (a measure of apoptosis). Similar to the cell cycle profile phenotypes, we observed an inhibition of pStat5 in the presence of V299L upon treatment with the collaterally sensitives, supporting an on-target ABL1 inhibition as the mechanism of action. (C) *In vitro* kinase assay at 10 μM ATP

with recombinant active ABL1 WT or V299L against vandetanib, showing a preferential inhibition of kinase assay against ABL1 V299L relative to WT. Results for other small molecules are shown in Supp Fig S6A. Data are shown as mean ± s.d. from three independent experiments. (D-E) Models of vandetanib docked to ABL1 WT and V299L. Vandetanib and bosutinib are shown in blue and orange, respectively. V299L causes steric hindrance to nitrile group of bosutinib, whereas it provides additional van der Waals contact to quinazoline group of vandetanib. See also Figure S5, S6, and S7.

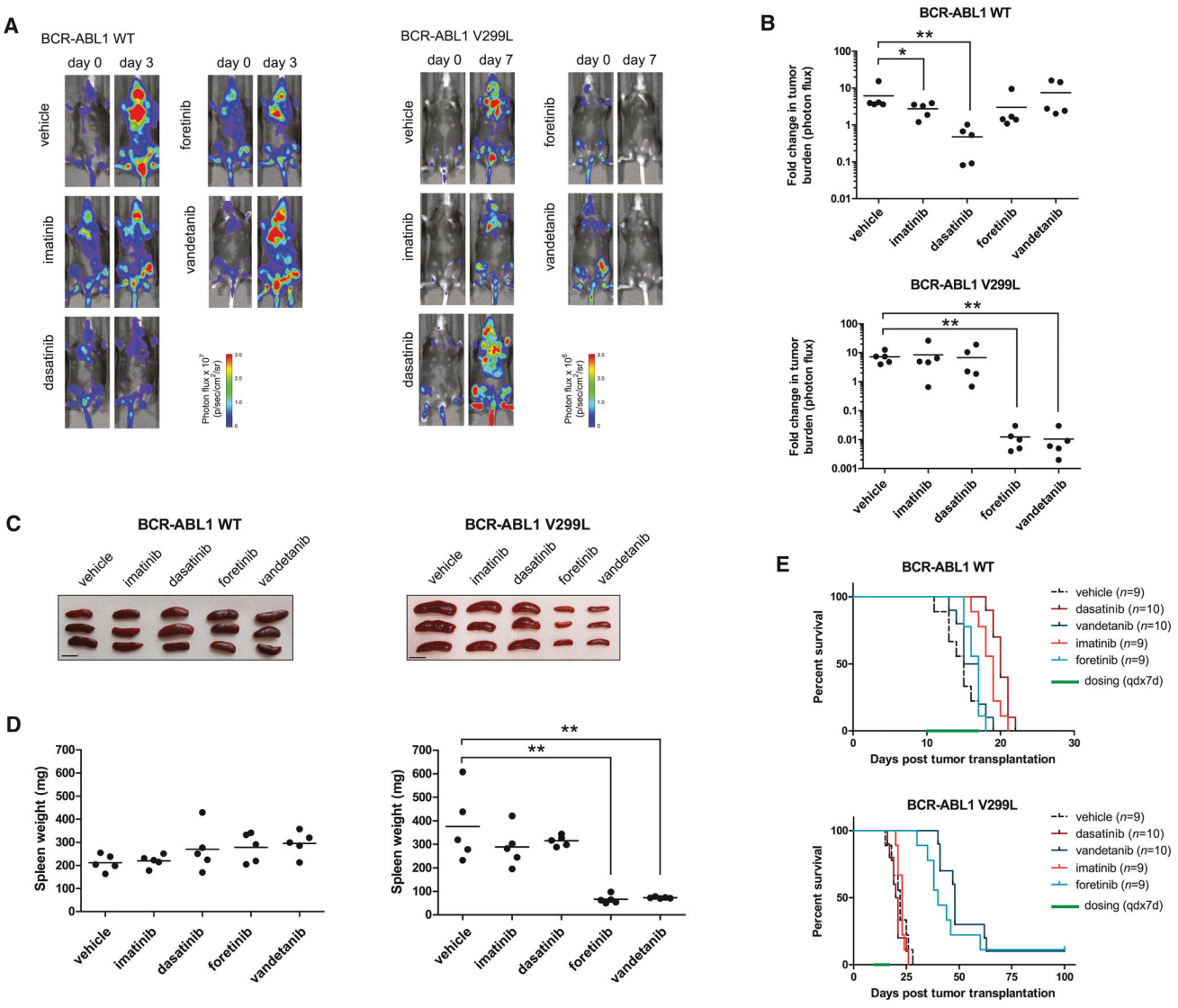

Figure 5. Non-canonical BCR-ABL1 inhibitors demonstrates *in vivo* efficacy

(A) Representative *in vivo* bioluminescence of mice at and during time of treatment. Derived cell lines with either BCR-ABL1 WT or V299L was tail-vein injected into immunocompetent recipient mice. Initial imaging was performed at day 10 post transplantation. Mice were subsequently treated once daily with vehicle, 10 mg/kg dasatinib, 50 mg/kg imatinib, 50 mg/kg vandetanib, or 50 mg/kg foretinib. (B) Fold change in total whole-mouse bioluminescence signal between post and pre- treatment. Mice bearing BCR-ABL1 V299L ALLs showed significant tumor burden reduction upon treatment with foretinib or vandetanib. Statistical significance determined by Mann-Whitney test. * $P <$ 0.05 and ** $P < 0.01$. (C–D) Spleen from the same cohort of mice was also imaged and weighted (4 days and 8 days post initial treatment for BCR-ABL1 WT and V299L, respectively). Treatment of BCR-ABL1 V299L *in vivo* with foretinib and vandetanib showed strong reduction in spleen size. Scale bar indicates 1 cm. Statistical significance determined by Mann-Whitney test. ** $P < 0.01$. (E) Kaplan-Meier overall survival of

immunocompetent recipient mice transplanted with BCR-ABL1 WT or V299L. Treatment of mice with foretinib or vandetanib led to significant extension in overall survival. Data presented was compiled from two independent injection experiments. Statistical significance determined with log-rank rest. *** $P < 0.001$.

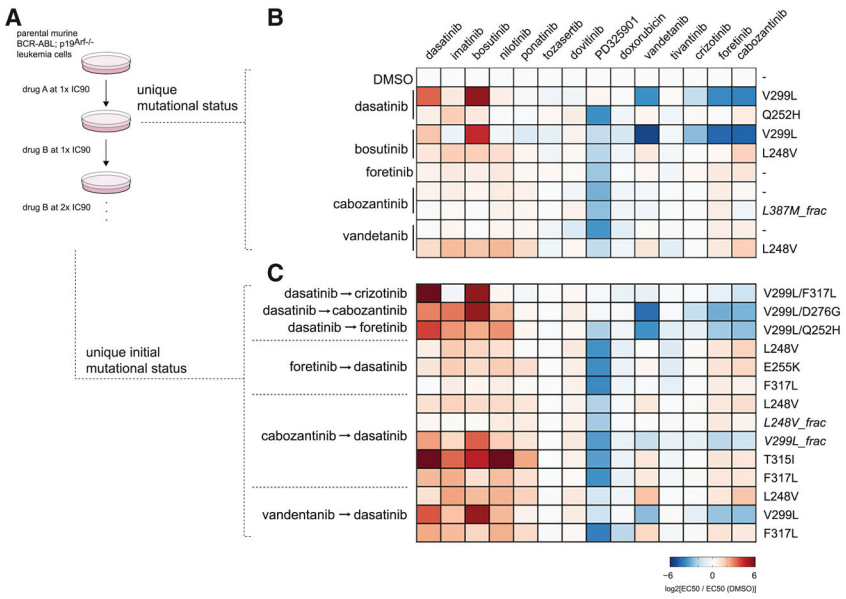

Figure 6. Sequential drug switching changes clonal trajectories. (A) Experimental setup of sequential drug selection

Parental ALL cell lines were initially selected with drug A at IC90 1x the concentration. Upon outgrowth, drug B was used at dose escalating concentrations for continued resistance selection. (B) Pharmacological profile depicting collateral resistance and/or sensitivity for recovered cells upon initial selection with drug A. Heatmap shows the log2 transform of the ratio in EC50s between given representative cell line with unique ABL1 mutation and the DMSO control cell line (similar as the parental). (C) Pharmacological profile for representative cell lines with initial unique ABL1 mutations following drug A → drug B selection. The sequence of drugs used for selection can diversify resulting resistant ABL1 mutations.

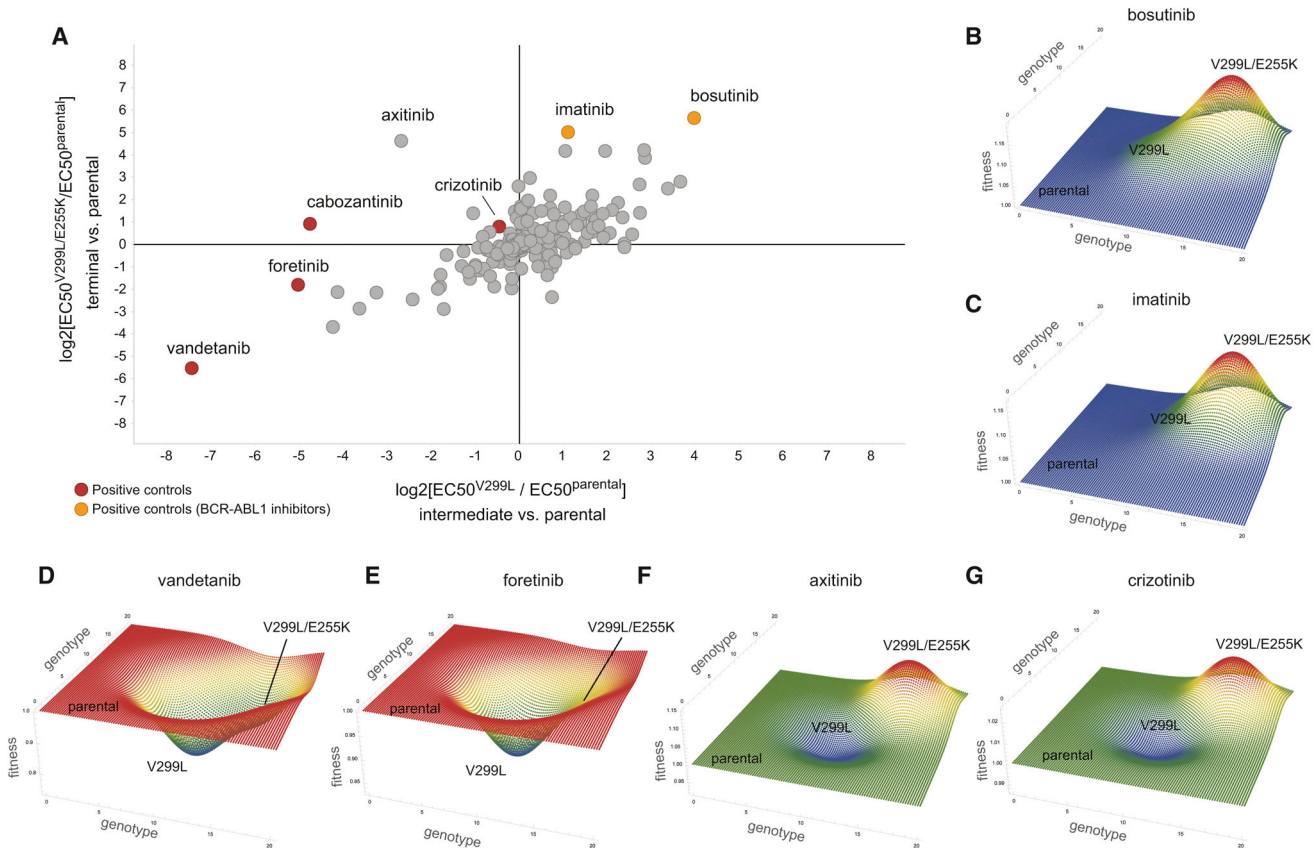

Figure 7. Small molecule screen reveals compounds with diverse fitness landscapes

(A) High-throughput small molecule screen with 391 compounds against parental, BCR-ABL1 V299L, BCR-ABL1 V299L/E255K derived ALL cell lines, as a model of the initial, intermediate, and terminal stages of clonal evolution. Plot shows the log2 ratio in EC50 between V299L and parental (for x-axis) and between V299L and V299l/E255K (for y-axis). Data points colored in orange are BCR-ABL1 inhibitor positive controls, and in red are other positive controls. (B–G) Conceptual fitness landscapes with predefined positions for the three clonal stages. Height of the peak/valleys determined based on actual EC50 values for given drug and cell line.